© Strojniški vestnik 48(2002)12,663-676
ISSN 0039-2480
UDK 66.063:66.069.82
Izvirni znanstveni članek (1.01)

© Journal of Mechanical Engineering 48(2002)12,663-676
ISSN 0039-2480
UDC 66.063:66.069.82
Original scientific paper (1.01)

# Metode prepoznave poplavnega stanja pri aeraciji v posodi s turbinskim mešalom

## Flooding-Recognition Methods in a Turbine-Stirred Vessel

**Andrej Bombač - Iztok Žun**

*V prispevku so obravnavane nekatere metode, s katerimi lahko na različne načine zaznamo poplavno stanje pri dispergiranju plina v kapljevino v posodi z enojnim Rushtonovim mešalom. To so metode merjenja splošnih veličin, npr. najmanjša moč mešala in največji prirastek plinaste faze ter metoda zaznave lokalnih karakteristik faznega stika. Preskus je potekal pri dispergiranju zraka v vodo ter delno pri dispergiranju zraka v vodno raztopino karboksi-metil-celuloze (KMC) različnih koncentracij. Prikazani sta medsebojna primerjava rezultatov ter primerjava z rezultati kriterijev drugih avtorjev.*

**(Ključne besede: mešala turbinska, stanja poplavna, metode prepoznavanja, dispergiranje zraka)**

*This article paper presents some appropriate methods for flooding detection by the dispersion of gases into liquids in a stirred vessel equipped with a single Rushton turbine. These methods are based on measurements of global properties, such as mixing-power minimum and gas-holdup maximum, and a method based on the local interfacial characteristics of two-phase systems. The experiments were performed by dispersing air into water and air partly into water-carboxy-methyl cellulose (CMC) solutions of different concentrations. A comparison of the results of the different methods is shown, as well as a comparison with the results from criteria found in the literature.*

**(Keywords: turbine-stirred vessel, flooding, recognition methods, air dispersion)**

## 0 UVOD

Pri dispergiranju plina v kapljevino v posodi z mešalom nastajajo na lopaticah mešala plinske votline, ki so osnovni mehanizem dispergiranja. V odvisnosti od količine dovedenega plina ($q$) in vrtilne frekvence mešala ($n$) ter od prenosnih lastnosti kapljevine nastajajo na lopaticah mešala različne strukture plinskih votlin. Z večanjem pretoka zraka pri stalni vrtilni frekvenci mešala lahko nastanejo naslednje strukture plinskih votlin [4]: struktura vrtinčno oprijemajočih se plinskih votlin (*VC*), struktura z eno veliko plinsko votlino (*1L*), struktura z dvema velikima plinskima votlinama (*2L*), struktura s tremi velikimi plinskimi votlinami (*S33*), struktura s tremi majhnimi in tremi velikimi plinskimi votlinami (*L33*) ter struktura raztrganih plinskih votlin (*RC*). Po viru [9] poteka dispergiranje na industrijskih napravah večinoma v režimu velikih plinskih votlin, tako da je pomembno poznavanje hidrodinamičnega režima, pri katerem lahko napovemo poplavno stanje. Po splošni definiciji poplavnega stanja, ki jo zasledimo v literaturi, je poplavno stanje predstavljeno kot prehod v neučinkovito delovanje mešala pri dispergiranju plina. Tako se z vidika struktur plinskih voltin pojavi poplavno stanje takrat, ko je na

## 0 INTRODUCTION

In the dispersing of air into water using stirrers in a mixing vessel, gas-filled cavities are formed behind each blade of the impeller, which represents the basic mechanism of dispersal. Depending on the air flow rate ($q$) and impeller rotational frequency ($n$), as well as liquid transport properties, various different gas-filled cavity structures are formed. By increasing the air flow rate at a constant impeller speed the following structures [4] can be formed: a vortex-clinging (*VC*) structure, a structure with one large cavity (*1L*), a structure with two large cavities (*2L*), a small '3-3' (*S33*) structure, a large '3-3' (*L33*) structure and ragged cavities (*RC*). According to Smith [9], dispersal with industrial-scale reactors mostly takes place in the large cavity regime, so the prediction of hydrodynamic regimes at which flooding occurs is of great importance. The general definition of flooding is often described in the literature as a transition to the unsatisfactory operation of an impeller in a gas-liquid system. Flooding occurred when an *RC* structure was detected in a particular location. Otherwise, flooding corresponded to the

opazovanem mestu zabeležena struktura raztrganih plinskih votlin, poplavno stanje pa je označeno z ustreznim hidrodinamičnim režimom ($n_F$, $q_F$).

Prispevek obravnava tri različne najpogosteje uporabljene eksperimentalne metode zaznave poplavnega stanja mešala pri dispergiranju zraka v posodi z Rushtonovim mešalom v vodi in v navidezplastični tekočini (karakteristike faznega stika). To so: metoda največjega prirastka deleža plinaste faze ([8] in [12]), metoda najmanjše moči mešala [7] in metoda zaznave karakteristik faznega stika ([6], [2], [4] in [5]). Iz medsebojne primerjave rezultatov teh metod je ugotovljeno, da je pri enostopenjskem mešalu poplavno stanje moč prepoznati z vsemi tremi metodami, rezultati se dobro ujemajo tudi z napovedanimi vrednostmi kriterijev drugih avtorjev.

## 1 POSKUS

### 1.1 Poskusna naprava

Poskus je bil izveden v pokončni valjasti posodi notranjega premera $T = 450$ mm z zaobljenimi robovi in ravnim dnom. V posodi, narejeni iz pleksi stekla, so bili osno simetrično nameščeni štirje motilniki toka, uporabljeno je bilo Rushtonovo mešalo s šestimi lopaticami. Shematski prikaz je podan na sliki 1. Uporabljeni so bili: demineralizirana voda, vodna raztopina KMC ter stisnjen zrak iz pnevmatskega voda pri sobni temperaturi. Podrobnejši opis geometrijskih parametrov mešalne posode in mešala je prikazan v delih [3] in [4].

hydrodynamic regimes marked with $n_F$ and $q_F$, where the impeller was no longer capable of dispersing all of the introduced air.

The purpose of this article is to present three different experimental methods of impeller-flooding recognition by air dispersing into water and air dispersing into a pseudoplastic fluid (interfacial characteristics) in a stirred vessel with a single Rushton turbine. These methods are: maximal gas holdup ([8] and [12]), minimal mixing power [7] and local detection of interfacial characteristics ([6], [2], [4] and [5]). Based on a comparison of the results of the given methods with single-impeller stirring it was found that the flooding state was easily recognized with all three methods. The results were in good agreement with the predicted data from the literature.

## 1 EXPERIMENT

### 1.1 Experimental setup

An experiment was performed in a cylindrical flat-bottomed Perspex vessel of diameter 450 mm with rounded edges and four baffles mounted perpendicularly to the vessel wall. A Rushton disk impeller with six blades was used. Demineralized water, a water solution of CMC and compressed air at room temperature were used in all experiments. The geometric details of the vessel and the impeller can be found elsewhere [3] and [4].

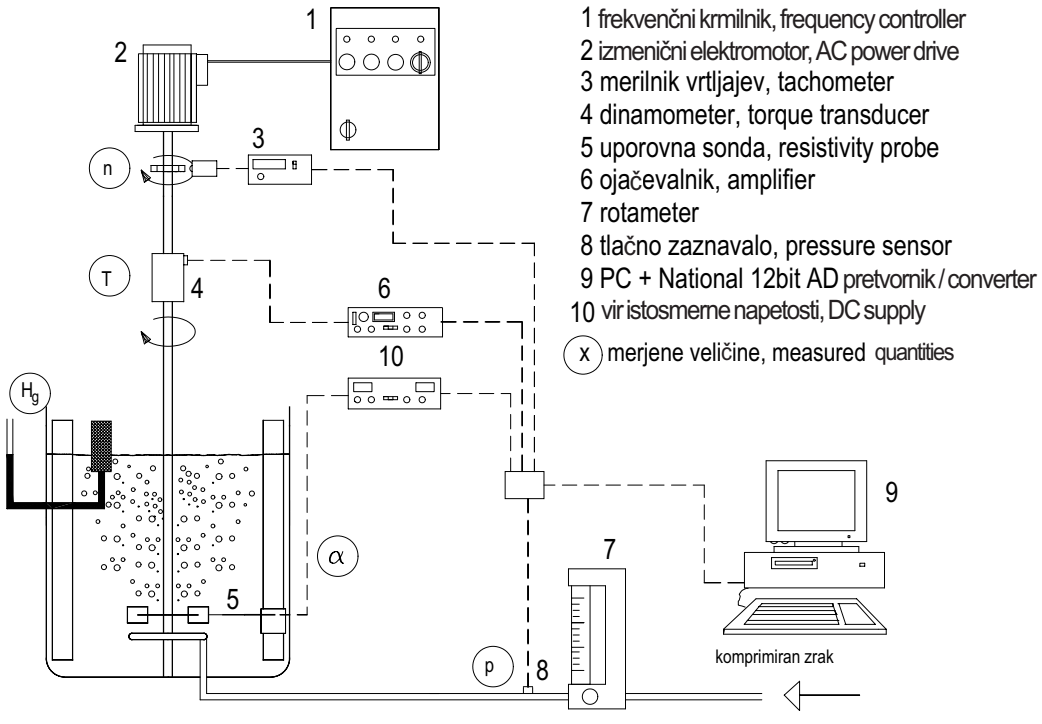


Sl. 1. *Merilna proga*
Fig. 1. *Experimental setup*

### 1.2 Merilna proga

Merilna proga je prikazana na sliki 1. Pogonski elektromotor je bil krmiljen s frekvenčnim krmilnikom, vrtilna frekvenca mešala je bila merjena s števnikom impulzov, ki deluje na načelu odboja lastnega signala z razredom točnosti 0,1. Vrtilni moment gredi je bil merjen z dinamometrom razreda točnosti 1, prostorninski pretok zraka z rotametrom razreda točnosti 2, z upoštevanjem poprave tlaka. Za omogočanje meritev večjih pretokov zraka sta bila vzporedno vezana dva rotametra. Celotni prirastek plinaste faze ($\alpha_g$) je bil merjen po načelu, opisanem v delu [8], prikazano na sliki 1. Zaznavalo gladine je bil nameščen na 2/3 radija posode.

Za obratovalne pogoje preskusne naprave so pri danih omejitvenih pogojih in točnosti merilne opreme izračunane tudi relativne napake naslednjih veličin [10]: največja merilna napaka momenta 16,1% (pri najnižjih vrtljajih), merilna napaka merjenja vrtilne frekvence 0,5%, relativna napaka merjenja temperature 0,5 %, relativna napaka merjenja tlaka s tlačnim zaznavalom 2%, relativna napaka Froudovega števila 1%, relativna napaka pretočnega števila 1,1% in relativna napaka globalnega deleža plinaste faze, manjša od 5%.

### 1.3 Metode zaznave poplavnega stanja

Za vse v nadaljevanju opisane metode je veljal enoten kriterij izvajanja meritev, po katerem so bile iskane veličine izmerjene pri nespremenljivi vrtilni frekvenci mešala ($n_i$ = konst) in postopnim majhnim povečevanjem pretoka zraka ($q_1$, $q_2$, $q_3$,...$q_{k-1}$, $q_k$). Pri vsaki nastavitvi ($n_i$, $q_j$), potem ko se je popolnoma razvil tok, so bile izmerjene višina gladine v posodi ($H_{g,i}$), moč mešala pri dispergiranju ($P_{g,i}$) ter strukturna funkcija ($M_{p,i}$). Pri nastavitvi na višjo vrtilno frekvenco mešala $n_2$, je bil postopek ponovljen.

#### *1.3.1 Metoda zmanjšanja moči*

Moč je bila izračunana iz izmerkov vrtilne frekvence in zaviralnega momenta mešalne osi. Na splošno se z večanjem pretoka plina pri dispergiranju moč mešala zmanjšuje in doseže najnižjo vrednost tik pred nastankom poplavnega stanja. Pri nastanku poplavnega stanja se moč mešala poveča, (sl. 2), kar so v svojih delih opisali ([7] ter [6]). Tako lahko poplavno stanje prepoznamo iz odvisnosti razmerja moči $\pi$ ($P_g/P$), ki se ob nastanku poplavnega stanja izrazito poveča. Tedaj plin mešalo obteka, mešalo pa zajema skoraj v celoti kapljevino, ki rotira znotraj dvigajočega se obročnega dvofaznega toka. Posledično se to kaže s povečanjem moči mešala. Takšen hidrodinamičen režim, pri katerem je zaznano poplavno stanje »označimo« kot ($q_F$, $n_F$), določeno posredno pri tisti vrednosti $(\pi_i)_F$, ko je bilo zadoščeno pogoju:

### 1.2 Measurements

The experimental setup is shown in Figure 1. The AC motor drive was controlled by a frequency controller, the impeller speed was measured with an infrared reflection counter of accuracy class 0.1. The impeller torque was measured using an in-line, precisely calibrated, HBM torque transducer of accuracy class 1. The volumetric air flow rates were measured by calibrated rotameters of accuracy class 2 , corrected for actual pressure. To enable measurements of larger air flow rates two rotameters were connected in parallel. The measurements of gas holdup ($\alpha_g$) were based on the change of the liquid height in the vessel using the method described in work of [8], see Figure 1. A level sensor was located at 2/3 of the tank radius.

The relative errors of the measured quantities were calculated for the working conditions of the experimental setup as follows [10]: maximum relative error of the torque at the lowest impeller speed was 16.1%, the relative error of the rotational speed was 0.5%, the relative error of temperature was 0.5%, the relative error of pressure was 2%, the relative error of the Froude number was 1%, the relative error of the Flow number was 1.1% and the relative error of the global gas holdup was less than 5%.

### 1.3 Flooding-recognition methods

For all the experimental methods described below the properties being investigated were always measured using the same principle. At a constant rotational impeller speed ($n_i$ = const) the surface level ($H_{g,i}$), the gassing mixing power ($P_{g,i}$) and the structural function ($M_{p,i}$) with successive small increases in air flow rate ($q_1$, $q_2$, $q_3$,...$q_{k-1}$, $q_k$) were taken. At each setting of ($n_i$, $q_j$) after a fully-developed regime was achieved, $H_{g,i}$ and $P_{g,i}$ were measured or $M_{p,i}$ recorded. After increasing the impeller speed to $n_2$, the procedure was repeated.

#### *1.3.1 Minimum mixing power*

The mixing power was calculated based on the rotational impeller speed and the mixing torque. In general, increasing the gas flow rate during dispersion reduces the mixing power and achieves the lowest value just before flooding occurs. When the impeller is flooded the mixing power increases, as shown in Figure 2, and described elsewhere [7], [6]. With this principle the power ratio curve described as $\pi = P_g/P$ can be used for flooding recognition. In such a regime the gas remains undistributed, the impeller is filled with liquid rotating inside an annular two-phase flow, which rises around the mixing shaft towards the free surface. Consequently, an increase in the mixing power takes place. The flooding regime ($q_F$, $n_F$) was determined indirectly by such a value of $(\pi_i)_F$ that fits the given condition:

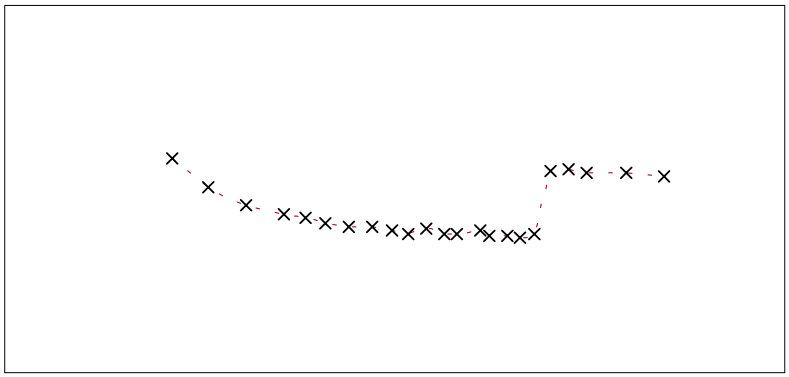


Sl. 2. *Odvisnost razmerja moči od vrtilne frekvence mešala pri nastanku poplavnega stanja*
Fig. 2. *Power ratio vs. impeller rotational frequency*

$$\frac{\pi_i - \pi_{i-1}}{Fl_i - Fl_{i-1}} \geq c_F \quad (1),$$

kjer so bile predhodno izmerjene vrednosti razmerij moči ($\pi_1, \pi_2, \pi_3, \ldots \pi_i \ldots \pi_{k-1}, \pi_k$), pri čemer je $c_F = 2$.

where ($\pi_1, \pi_2, \pi_3, \ldots \pi_i \ldots \pi_{k-1}, \pi_k$) were previously measured power ratios, and $c_F = 2$.

*1.3.2 Celotni delež plinaste faze*

Celotni delež plinaste faze je bil podan z razmerjem med prirastkom prostornine zaradi vnesene plinaste faze in celotno prostornino dvofaznega sistema, kar je lahko za posodo nespremenljivega prereza prevedeno v razmerje višin:

*1.3.2 Maximum gas holdup*

Global gas holdup was defined by the ratio between the gas phase and the liquid phase volume that can be transformed into a ratio of heights as follows:

$$\alpha_g = \frac{H_g - H}{H_g} \quad (2),$$

kjer pomenijo: $H_g$ – višino gladine dvofaznega sistema pri dispergiranju in $H$ – višino gladine vode pri mešanju brez dovajanja zraka. S povečevanjem vnosa plina v posodo se viša tudi gladina dvofaznega sistema do neke mejne vrednosti, ki je povzročena z nastankom poplavnega stanja. Pri prehodu iz dispergirnega v poplavno stanje se pojavi opazno znižanje gladine, kakor je prikazano na sliki 3. Do te spremembe pride zaradi izrazito nehomogene porazdelitve plinaste faze po prostornini kapljevine, tako v kapljevini pod mešalom ni obtekanja dvofaznega toka. Za določitev hidrodinamičnega režima poplavnega stanja ($q_F, n_F$) je bil uporabljen kriterij, ko je bilo pri vrednosti $(\alpha_i)_F$ zadoščeno pogoju:

where $H_g$ means the height of the two-phase free surface during dispersion and $H$ is the liquid height in single-phase mixing. Increasing the air flow rate during dispersion increases the gas holdup correspondingly, until flooding occurs. In the flooding transition a remarkable reduction of gas holdup can be seen, as depicted in Figure 3. This change can be explained by the extremely non-uniform distribution of gas in the liquid bulk, where, especially below the impeller, there was no two-phase circulation. The flooding regime ($q_F, n_F$) was determined indirectly by such a value of $(\alpha_i)_F$ that fits the given condition:

$$\frac{\alpha_i - \alpha_{i-1}}{Fl_i - Fl_{i-1}} \geq \left| c_F \right| \quad (3),$$

vrednosti celotnih deležev plinaste faze ($\alpha_{g,1}, \alpha_{g,2}, \ldots \alpha_i, \ldots \alpha_{g,k-1}, \alpha_{g,k}$) so bile predhodno izmerjene.

where the values ($\alpha_{g,1}, \alpha_{g,2}, \ldots \alpha_i, \ldots \alpha_{g,k-1}, \alpha_{g,k}$) were previously measured.

*1.3.3 Metoda karakteristik faznega stika*

Mehanizem dispergiranja je tesno povezan s strukturami plinskih votlin na lopaticah mešala [4]. S povečevanjem pretoka zraka se povprečna gostota izstopajočega dvofaznega toka iz mešala manjša, kakor tudi moč mešala, vse dokler se ne pojavi poplavno stanje [13]. Za lokalno zaznavo plinskih votlin za lopaticami mešala je bila že

*1.3.3 Interfacial characteristic method*

The dispersing mechanism is closely connected with the different structures of gas-filled cavities that are present at the impeller blades, as described in [4]. With increasing the air flow rate the average density of the discharge two-phase flow decreases (as well as the impeller power) until flooding occurs [13]. For local detection of the gas-filled cavity behind the impeller blade a previously

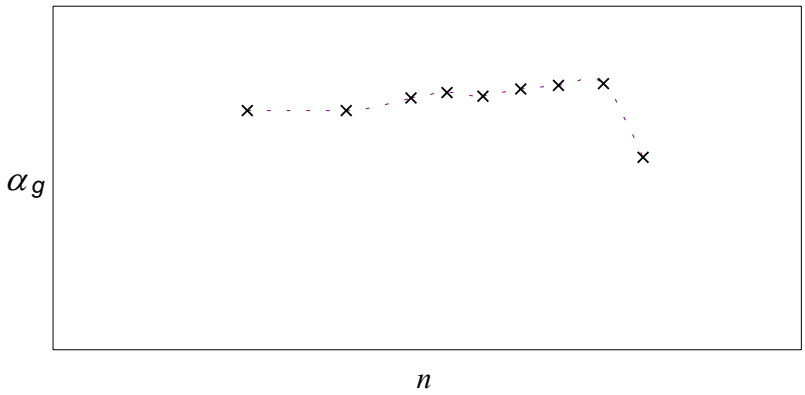


Sl. 3. *Odvisnost celotnega deleža plinaste faze od vrtilne frekvence mešala*
Fig. 3. *Global gas holdup vs. impeller rotational frequency*

poprej razvita preskusna metoda karakteristik faznega stika. Velika razlika v električni upornosti vode in zraka je osnovna lastnost, ki jo z uporovno sondo zaznamo in pomeni odziv sonde v obliki električne napetosti, oziroma ustrezno strukturno funkcijo:

developed experimental method based on local interfacial characteristics was used. A remarkable difference in the electrical resistance of the water and the air is a basic property, which can be detected using a resistivity probe and presented as a probe voltage response or corresponding structural function $M_p$ defined as:

$$M_p(x,t) = \begin{cases} 1, & x \text{ je v fazi / is in phase } p \\ 0, & x \text{ ni v fazi / is not in phase } p \end{cases} \qquad p = \{L, G, S\} \tag{4}$$

kjer so v področju dvofaznega toka na mestu $x$ ter v času $t$ mogoča tri stanja $p$: $L$ kapljevita faza , $G$ plinasta faza in $S$ stična površina.

Frekvenčna analiza strukturne funkcije $M_p$ z diskretno Fourierjevo preslikavo omogoča prikaz značilnih frekvenc pojavljajoče se plinaste faze. Fourierjevi koeficienti so bili določeni iz:

where in a two-phase flow field three states $p$ are possible at a particular point $x$ at any time $t$: the liquid phase $L$, the gas phase $G$ or the phase interface $S$.

A frequency analysis of the structural function $M_p$ with a discrete Fourier transformation enabled the presentation of the significant frequencies of an appearing gas phase. The Fourier coefficients $X_k$ were obtained from:

$$X_k = \Delta t \sum_{k=0}^{N-1} M_p(t_k) e^{-\frac{j2\pi ik}{N}} \tag{5},$$

kjer pomeni $\Delta t$ časovni korak med vzorcema diskretne funkcije. Med Fourierjevimi koeficienti $X_k$, ki se ujemajo s frekvenco $k/(N\Delta t)$, so veljavni le koeficienti med $k = 0$ to $k = N/2 - 1$. Kriterij prepoznave struktur plinskih votlin je podrobneje opisan v delu [4], ter omogoča pri mešanju z Rushtonovim mešalom prepoznavo naslednjih struktur: vrtinčno oprijemajoča struktura plinskih votlin (*VC*), struktura z eno veliko plinsko votlino (*1L*), struktura z dvema velikima plinskima votlinama (*2L*), struktura s tremi velikimi plinskimi votlinami (*S33*), struktura s tremi majhnimi in tremi velikimi plinskimi votlinami (*L33*) ter struktura raztrganih plinskih votlin (*RC*). Značilni vzorci struktur v frekvenčnem prostoru so prikazani na sliki 4. Kakor je videti iz razvoja struktur, je zadnja značilna struktura, struktura raztrganih plinskih votlin, ki pripada poplavnemu stanju. Po viru [11] se stabilna struktura L33 vrne v strukturo šestih simetričnih oprijemajočih se plinskih voltin, pri višjih vrtilnih frekvencah mešala pa se prehod naredi prek strukture s šestimi velikimi plinskimi votlinami enake velikosti, ki so opisane kot silovito vibrirajoče votline oziroma raztrgane votline [7].

where $\Delta t$ denotes the time interval between successive instants $t_i$. Among the Fourier coefficients $X_k$ that correspond to the frequency $k/(N\Delta t)$, only the coefficients from $k = 0$ to $k = N/2 - 1$ are meaningful. The criterion for gas-filled cavity-structure recognition was described in detail in [4], as were the recognized structures: a vortex-clinging (*VC*) structure, a structure with one large cavity (*1L*), a structure with two large cavities (*2L*), a small '3-3' (*S33*) structure, a large '3-3' (*L33*) structure and ragged cavities (*RC*). A significant pattern of the structures in a frequency domain is depicted in Figure 4. The last evident structure, as can be seen from the evolution of the frequency domain, is the ragged cavities structure, and corresponds to the flooding state. According to the literature [11] the stable L33 structure reverts to six symmetrical clinging cavities; at higher impeller speeds the transition occurs through a regime with six large cavities of identical size, which are described as violently vibrating, i.e. ragged cavities [7].

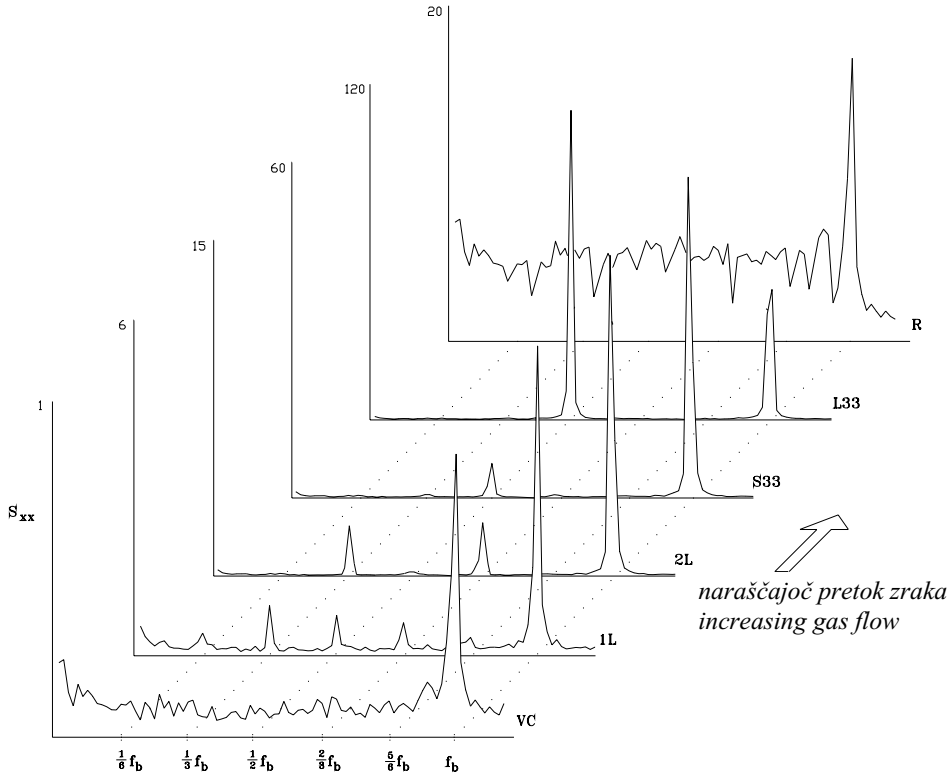


Sl. 4. *Razvoj struktur plinskih votlin ob postopnem večanju pretoka zraka. Poplavno stanje je določeno s pojavom strukture raztrganih plinskih votlin.*
Fig. 4. *Gas-filled cavity structure development with incremental increase of gas flow. Flooding is determined with the appearance of ragged cavity structure.*

## 2 ANALIZA REZULTATOV IN PRIMERJAVA

### 2.1 Nastanek poplavnega stanja pri dispergiranju zraka v vodi

#### *2.1.1 Metoda celotnega deleža plinaste faze*

Nastanek poplavnega staja je opažen pri tisti vrednosti pretočnega števila, pri kateri se pojavi opazno znižanje gladine dvofaznega sistema, oziroma celotnega deleža plinaste faze. Na podlagi spremembe gladine lahko prepoznamo poplavna stanja le za vrednosti *Fr* od 0,05 do 0,6. Na sliki 5 so prikazane vrednosti $\alpha_g$ pri *Fr* = 0,05 do 0,13 v odvisnosti od *Fl*. Vidno je enakomerno zvečanje deleža plina pri povečevanju vnosa zraka, sledi močno zmanjšanje vrednosti v točki poplavnega stanja. Pri nadaljnjem večanju pretoka zraka se zaradi večjih mehurčkov in večje količine plina v stebru plina okoli mešalne osi gladina lahko znova rahlo zviša, kar pa je z vidika učinkovitosti zaradi zrazito nehomogene porazdelitve plinaste faze neučinkovita operacija. Na sliki 6 so prikazane vrednosti $\alpha_g$ pri *Fr* = 0,2 do 0,6 v odvisnosti od *Fl*. Tudi tu so lepo vidna zmanjšanja vrednosti v točkah poplavnega stanja. Pri večjih vrednostih *Fr*>0,7 je vnesena količina zraka že tako velika, da se pojavlja močno nihanje gladine s 'pljuskanjem' vode, kar je za odbiranje višine gladine nezanesljivo. Tudi

## 2 RESULTS ANALYSIS AND COMPARISON

### 2.1 Flooding in air dispersing into water

#### *2.1.1 Maximum gas holdup method*

In this method the flooding is detected by the particular flow number, where there is a rapid decrease of surface level or gas holdup. Based on the free-surface level change only flooding states at Froude numbers between 0.05 and 0.6 can be recognized. In Figure 5 the dependence of $\alpha_g$ on *Fl* at given *Fr* = 0.05 to 0.13 is depicted. A reasonable increase of $\alpha_g$ can be seen, with its dependence on the increasing flow number, followed by a rapid reduction of $\alpha_g$ in the flooding regime. With further enlargement of the air input the surface level can be a little higher than that in the flooding state, probably due to large air bubbles that rise upwards to the surface around the mixing shaft like a slug flow. Such an extreme non-homogeneous distribution can be described from the efficiency aspect as an unsatisfactory operation. Depicted in Figure 6 is the dependence of $\alpha_g$ on *Fl* at *Fr* = 0.05 to 0.13. Again a decrease of $\alpha_g$ can be seen in the flooding state. At higher values, at *Fr*>0.7, a waving of the free surface occurred so the relevant readings were no longer possible. Otherwise,

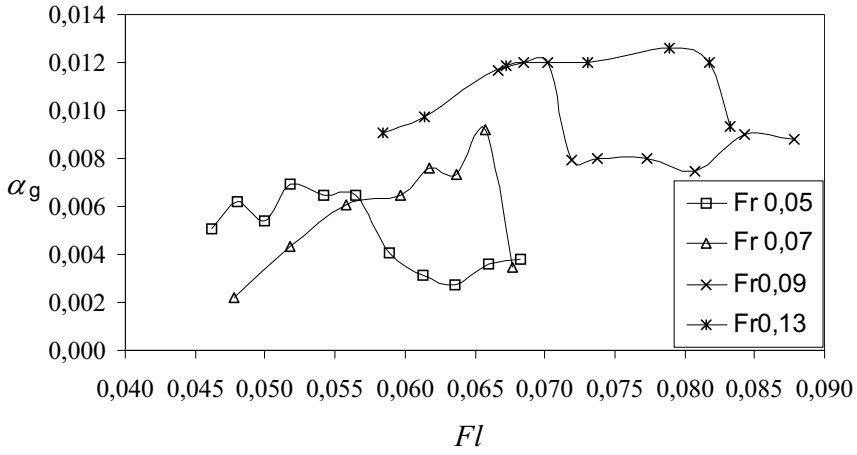


Sl. 5. *Prirastek celotnega deleža plinaste faze v odvisnosti od Froudovega in pretočnega števila*
Fig. 5. *Global gas holdup vs. Froude and Flow number*

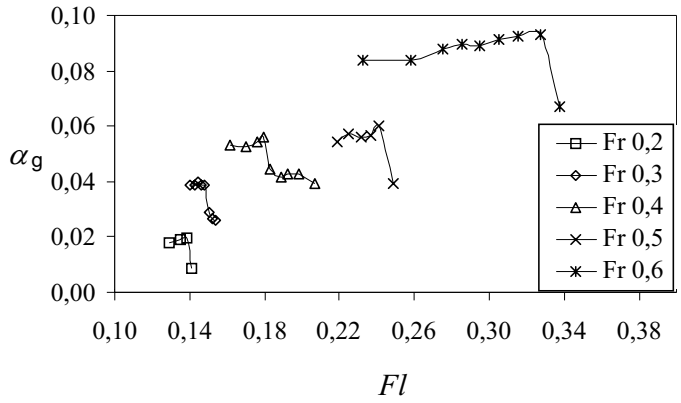


Sl. 6. *Prirastek celotnega deleža plinaste faze v odvisnosti od Froudovega in pretočnega števila*
Fig. 6. *Global gas holdup vs. Froude and Flow number*

sicer pri nastanku poplavnega stanja v mešalniku težko zaznamo gladino dvofaznega sistema, kar se kaže tudi z večjo napako izmerka.

V literaturi [11] in [7] so razmejitvene črte različnih struktur dvofaznih tokov običajno prikazane v tokovni mapi, diagramu, izraženem z brezizmernimi števili *Fr* in *Fl*. V diagramu 7 so vnesene vrednosti, ki ustrezajo prepoznavnim poplavnim stanjem. Razmejitvena črta poplavnega stanja je podana z ustrezno poenostavitveno premico, katere koeficienti so prikazani v preglednici 1.

readings of $H_g$ in all flooding states were difficult to detect precisely, which was reflected in a higher relative error of $\alpha_g$.

Usually the delineation line between the dispersing and flooding regimes is depicted in a flow regime map expressed with dimensionless *Fr* and *Fl* numbers, such as the one found in the literature [11] and [7]. In Figure 7 all the recognized flooding regimes ($n_F$, $q_F$ ) given by this method are indirectly shown through *Fr* an *Fl* numbers. Based on this data the flooding line is approximated by Equation 6, coefficients $k_1$ and $k_2$, and the regression coefficient *r*; all are given in Table 1.

Preglednica 1. *Pripadajoči koeficienti k enačbi [6]*
Table 1: *Corresponding coefficients to Eq. [6]*

| metoda<br>method | $k_1$ | $k_2$ | $r$ |
|---|---|---|---|
| celotni prirastek plinaste faze<br>global gas holdup | -0,54 | 2,1 | 0,96 |
| najmanjši porast moči<br>minimal mixing power | 0,05 | 1,5 | 0,97 |
| značilnica faznega stika<br>interfacial characteristics | 0,33 | 1,4 | 0,96 |

*2.1.2 Metoda zmanjšanja moči*

S to metodo so potekale meritve poplavnega stanja pri vrednostih *Fr* od 0,05 do 1,13. Na slikah 8 in 9 so podane tipične krivulje razmerja moči $P/P_0$, pri katerem je v poplavnem stanju opazno zvečanje razmerja moči. Pri manjših vrednostih *Fr* (0,05, 0,06, 0,07 in 0,09 na sliki

*2.1.2 Minimum mixing power*

According to this method the measurements were taken at *Fr* numbers from 0.05 to 1.13. Typical curves of the power ratio $P/P_0$ are depicted in Figures 8 and 9, where a steep increase of the power ratio during the flooding state can be seen. On the other

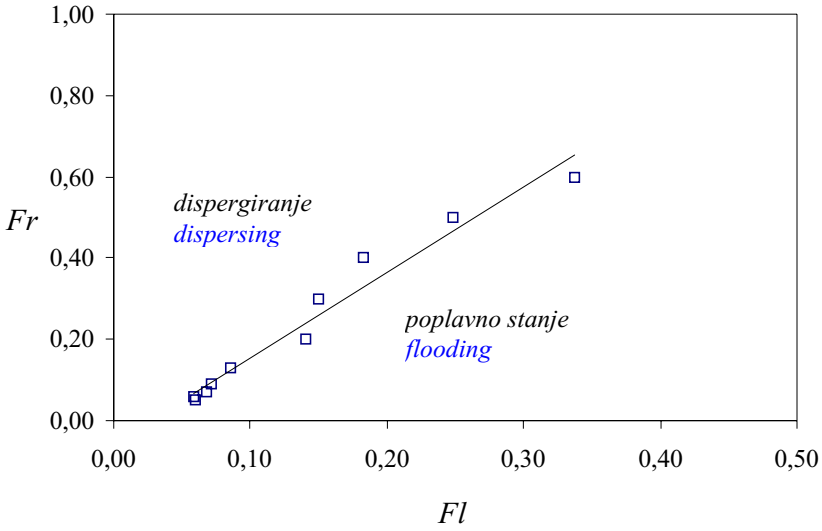


Sl. 7. *Točke poplavnega stanja določene z metodo celotnega deleža plinaste faze v tokovnem diagramu z mejo poplavnega stanja*

Fig. 7. *Flooding points determined by global gas holdup method on a flow chart with approximated flooding limit*

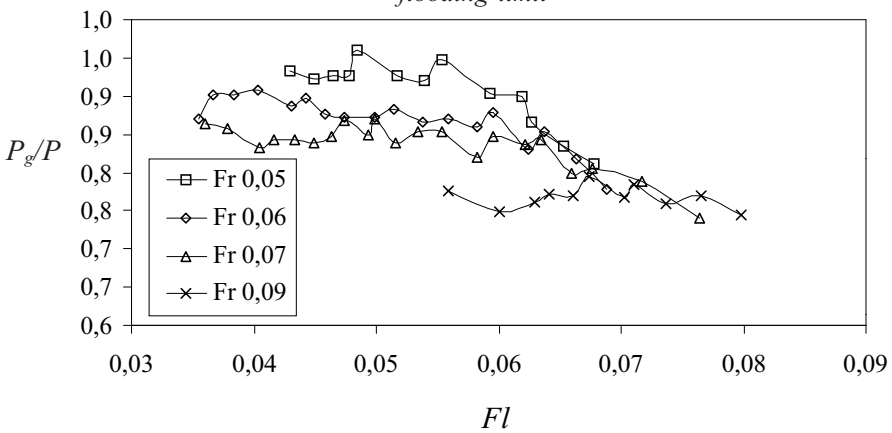


Sl. 8. *Odvisnost razmerja moči od pretočnega števila pri različnih vrednosti Froudovega števila*

Fig. 8. *Power ratio vs. Flow number at different Froude number values*

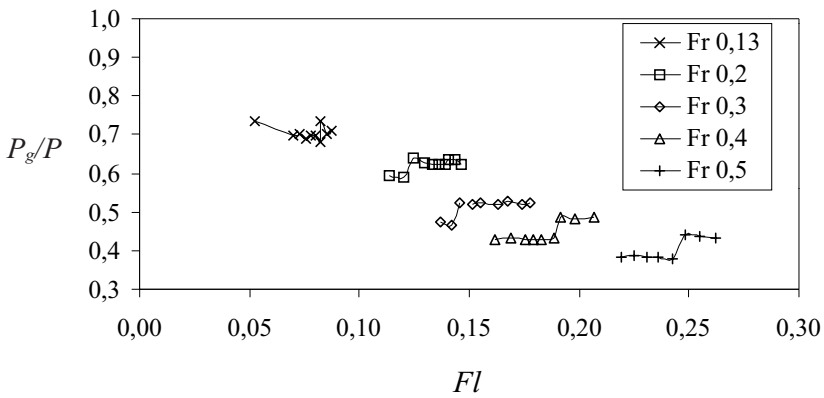


Sl. 9. *Odvisnost razmerja moči od pretočnega števila pri različnih vrednosti Froudovega števila*

Fig. 9. *Power ratio vs. Flow number at different Froude number values*

8) metoda ni dala pomembnih rezultatov. Razlog je lahko v premajhni moči mešala, saj so izmerki vrtilnega momenta mešala enakega velikostnega razreda kakor odstopki merilnika vrtilnega momenta. V diagramu, prikazanem na sliki 11, so podane vse z metodo zmanjšanja moči prepoznane točke poplavnega stanja. Podana je tudi ustrezna razmejitvena premica, katere koeficienta $k_1$ in $k_2$ in poenostavitveni koeficient $r$ so prikazani v preglednici 1.

*2.1.3 Metoda karakteristik faznega stika*

Iz postopnega razvoja značilnih vzorcev struktur plinskih votlin v frekvenčnem prostoru (sl. 4) za vsako nastavitev parametrov hidrodinamičnega režima ($n$=*konst,* $q_j$), je lepo razviden nastanek strukture raztrganih plinskih votlin, ki ustreza poplavnemu stanju. Režimi ($n_F$, $q_F$), prepoznani kot poplavno stanje, so bili v obliki brezizmernih števil *Fl* in *Fr* vneseni v diagram na sliki 12. Izmerjene vrednosti so predstavljene z ustrezno razmejitveno premico, katere koeficienti so prikazani v preglednici 1.

*2.1.4 Medsebojna primerjava rezultatov različnih metod*

Pri meritvah so se glede na uporabljeno metodo in merilna oprema pojavile nekatere omejitve. Tako z metodo prirastka deleža plinaste faze ni bilo mogoče določiti poplavnega stanja predvsem pri večjih pretokih zraka, medtem ko z metodo zmanjšanja moči predvsem pri nižjih pretočnih številih. Z metodo karakteristik faznega stika je bilo mogoče prepoznati poplavno stanje v celotnem območju merjenih režimov. Za prepoznavna poplavna stanja, določena z vsemi tremi metodami, so bile izdelane ustrezne razmejitvene premice, podane z enačbo:

hand, this method did not give any relevant results for smaller *Fr* numbers (0.05, 0.06, 0.07 and 0.09 in Figure 8), which can be explained with the very small values of the impeller power and are of the same scale as the dynamometer´s accuracy class. All the recognized flooding regimes are depicted in Figure 11, together with the corresponding correlated delineation line; the appropriate coefficients $k_1$ and $k_2$ and the regression coefficient $r$ are given in Table 1.

*2.1.3 Interfacial characteristic method*

From the coherent development of the structure patterns in a frequency domain, as shown in Figure 4, the appearance of the ragged cavities structure can be found for each hydrodynamic regime set ($n$=*const,* $q_j$). The corresponding flooding regimes ($n_F$, $q_F$) were collected and are shown in the form of dimensionless *Fr* and *Fl* numbers in a flow regime map, see Figure 12, as well as a flooding line approximated in the form of eq. 2. The corresponding coefficients are given in Table 1.

*2.1.4 Comparison of results of different methods*

According to the methods used and the measuring instrumentation, some restrictions appeared. Flooding could not be recognized at higher air flow rates with the global-gas-holdup method and at lower gas flow rates with the minimum-mixing-power method. Using the interfacial characteristics method gave relevant recognition of the flooding in all the measured regimes. For all the recognized flooding states with the given methods, the corresponding regression lines were approximated by the equation:

$$Fr_F = k_1 + k_2 \cdot Fl_F \qquad (6).$$

Vrednosti posameznih koeficientov so prikazane v preglednici 1.

Individual values of the coefficients are given in Table 1.

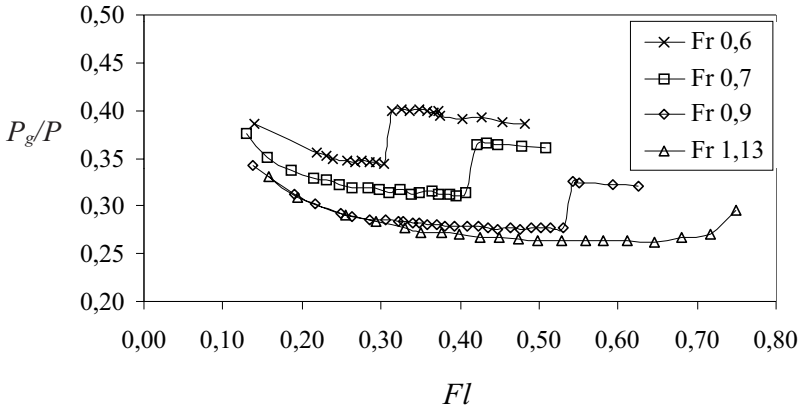


Sl. 10. *Odvisnost razmerja moči od pretočnega števila pri različnih vrednosti Froudovega števila*
Fig. 10. *Power ratio vs. Flow number at different Froude number values*

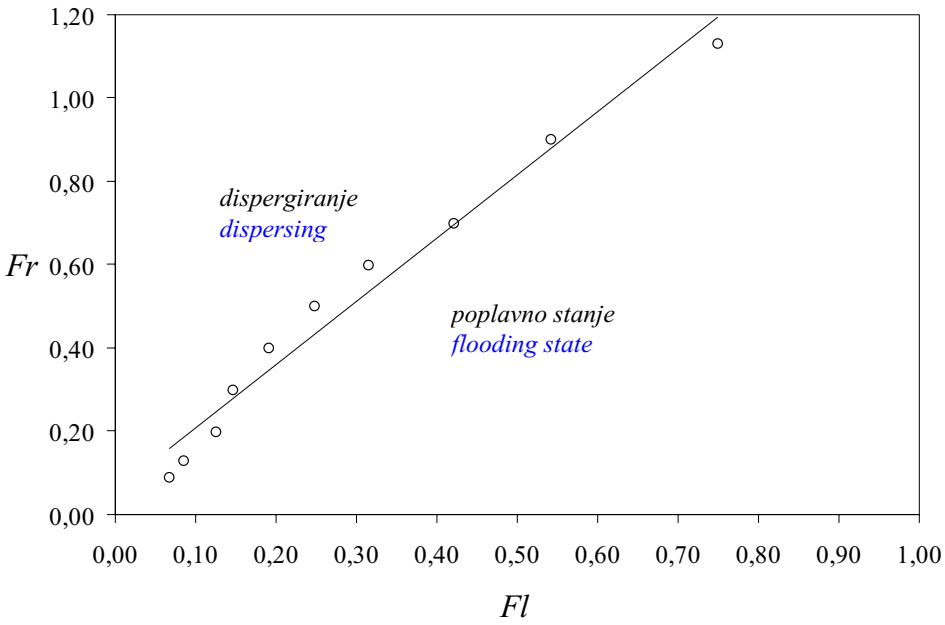


Sl. 11. *Točke poplavnega stanja določene z metodo razmerja moči v tokovnem diagramu z mejo poplavnega stanja*

Fig. 11. *Flooding points determined by power ratio method on a flow chart with approximated flooding limit*

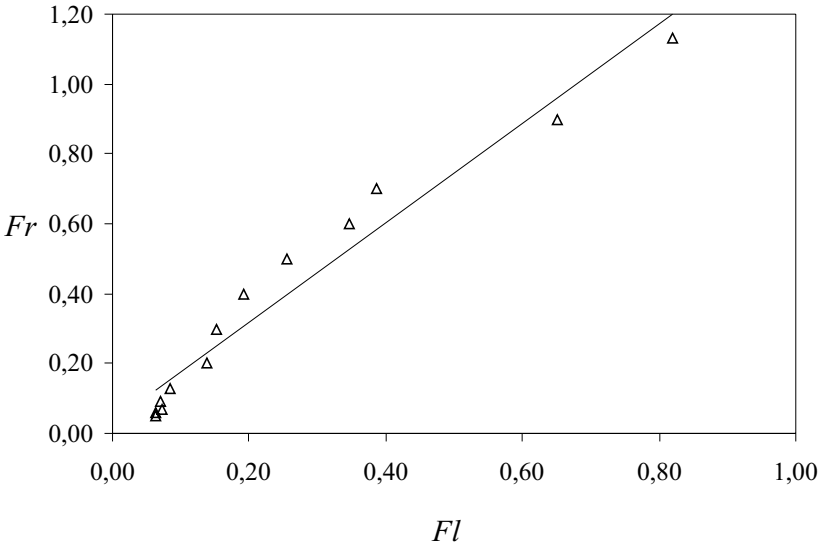


Sl. 12. *Točke poplavnega stanja določene z metodo karakteristik struktur faznega stika v tokovnem diagramu z mejo poplavnega stanja*

Fig. 12. *Flooding points determined by local characteristics method on a flow chart with approximated flooding limit*

Primerjava rezultatov kaže, da so vse tri metode primerne za določitev poplavnega stanja mešala. Pri nižjih vrednosti *Fr* in *Fl* je medsebojno razhajanje manjše med metodami celotnega prirastka deleža plinaste faze in karakteristikami faznega stika. Glede na strmino pripadajočih poenostavitvenih premic je boljše ujemanje med metodama karakteristik faznega stika in najmanjše moči mešanja.

Pri dispergiranju plina z enim mešalom se lokalne spremembe na lopaticah mešala in v neposredni okolici mešala kažejo enoznačno tudi na celotni ravni. Pri poplavnem stanju mešala se torej

A comparison of the results showed that all three methods are suitable for flooding detection. The smallest differences can be seen at the smaller values of *Fr* and *Fl* between the global-gas-holdup method and the interfacial characteristics method. According to the trend, better agreement can be found between the minimum mixing-power and the interfacial characteristics methods.

In gas dispersing with one impeller, the local changes at the impeller blades and in the close vicinity of the impeller affect the global level directly. In impeller flooding the global change is expressed

celotna sprememba izraža kot zmanjšanje celotnega deleža plina oziroma kot povečanje moči mešala. Poraja se vprašanje, ali je mogoče zaznati poplavno stanje pri dispergiranju z dvema mešaloma ali tremi mešali s katerokoli celotno metodo, kar ostaja odprto vprašanje za nadaljnje raziskave.

*2.1.5 Primerjava rezultatov z napovedanimi po virih iz literature*

Rezultati naših raziskav so bili primerjani tudi z rezultati kriterijev drugih avtorjev, kar je prikazano na sliki 13. Primerjani so le kriteriji, ki obsegajo tudi geometrijska razmerja in velikostni razred reaktorja kakor v naši raziskavi pri dispergiranju z enim Rushtonovim mešalom. Po [12], kriterij izhaja iz meritev prirastka deleža plinaste faze, je meja poplavnega stanja v reaktorju pri $D/T$ = 1/3 definirana z vrtilno frekvneco mešala ter pretokom plina v obliki:

through a reduction of the gas holdup or an increase of the minimum mixing power. The question appears, whether it is possible to detect flooding by dispersing with dual or triple impellers using any of the mentioned global methods? This remains open for further research.

*2.1.5 Comparison of the results with those quoted from the literature*

The results of our experiments were compared with those based on the correlations of other researchers, as can be seen in Figure 13. Only the criteria including the geometrical ratios between the impeller and the tank diameter and reactor-size scale were taken for a comparison with the experimental results during dispersion with a single Rushton turbine. According to [12], these criteria are derived from global-gas-holdup measurements, a flooding regime at a $D/T$ ratio equal to 1/3 is defined with impeller speed and gas flow rate in the form:

$$n_F = 2{,}694 \cdot q_F^{\,0{,}283} \cdot T^{-1{,}207} \quad (7).$$

Nienow [7] je postavil povezavo, ki zajema tudi različna geometrijska razmerja med mešalom in posodo ($1/3 \le D/T \le 2/3$) ter velikostni razred posode ($0{,}29 \le T \le 1{,}2$ v m):

Nienow [7] postulated a correlation including different geometrical ratios ($1/3 \le D/T \le 2/3$) as well as reactor scale size ($0{,}29 \le T \le 1{,}2$ [m]):

$$Fl_F = 30\,(D/T)^{3,5}\,Fr_F \quad (8).$$

S slike 13 je razvidno dobro ujemanje vrednosti napovedi naših meritev po metodi najmanjše moči mešnja in metodi karakteristik faznega stika z napovedjo po [7]. Glede na to, da so njihove vrednosti v pasu znotraj naših, to potrjuje Nienowo kombinacijo kriterijev porasta moči mešanja ter opazovanja tokovnih struktur, ko je bil postavljen omenjeni kriterij (en. 8). Iz primerjave metod na temelju celotnega prirastka plinaste faze se težnja naših vrednosti v izmerjenem področju dobro ujema z vrednostmi po [12], sicer pa je poplavno stanje v našem primeru doseženo pri nekoliko višjih vrednostih pretočnega števila.

In Figure 13, good agreement can be seen between our predicted values, based on the minimum-mixing-power method and the interfacial characteristics method with those predicted by Nienow. Regarding the fact that the values given with Eq. 8. appear in between ours, the assumption of their criterion postulated on the combination of the minimum-mixing-power and flow-structure methods can be confirmed. From the comparison of the results based on the global-gas-holdup method, the trend of our values is in a good agreement with those of [12] in the measured range, otherwise the flooding was achieved at slightly higher values of *Fl* number.

**2.2 Nastanek poplavnega stanja pri dispergiranju zraka v raztopini KMC**

Dispergiranje zraka v vodni raztopini KMC je potekalo z Rushtonovim mešalom. Ta preskus je bil izveden na isti merilni progi, izsledki obravnavani v tem prispevku pa izhajajo iz študije struktur plinskih votlin objavljene v delu [3].

Strukture plinskih votlin so bile predstavljene v diagramu struktur, izraženem z brezrazsežnimi števili *Fr-Fl*. Plinske votline so v navidezplastični kapljevini večje od teh v vodi in imajo drugačno obliko, opazen je bil tudi pojav, pri katerem ostanejo plinske votline na lopaticah mešala še po zaprtju dovoda zraka. Pri navidezno

**2.2 Flooding in air dispersing into pseudoplastic fluid CMC**

Dispersing of air into a pseudoplastic fluid of water-diluted CMC was performed with a single Rushton impeller using the same experimental setup. The results discussed here are derived from a gas-filled-cavity-structure study published elsewhere [3].

The structures were classified in a flow-regime map given with *Fr-Fl* dependency. The gas-filled cavities in a CMC solution are larger than those in water, and have a rather different shape. A phenomenon was also found whereby gas-filled cavities were present at the impeller blades for a longer time of observation, even after the air inflow was closed.

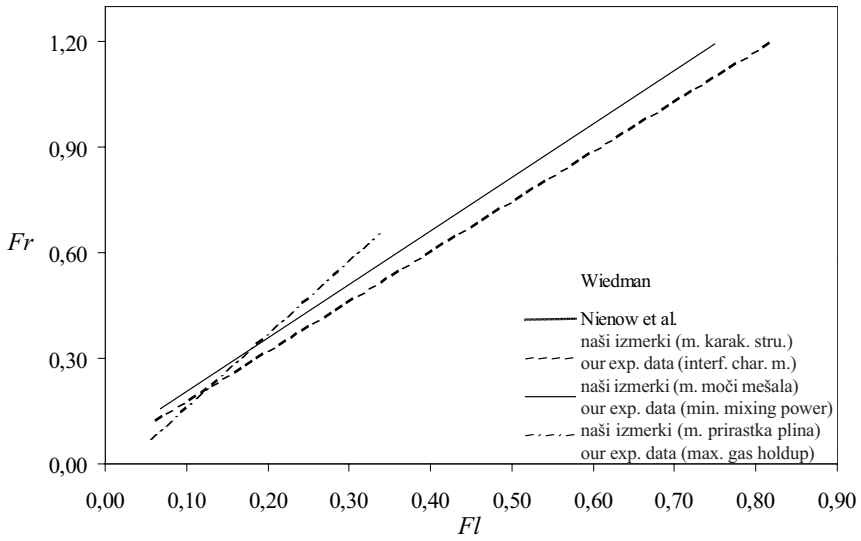


Sl. 13. *Primerjava meja poplavnega stanja z rezultati drugih avtorjev*
Fig. 13. *Comparision between our results and calculated values by other authors*

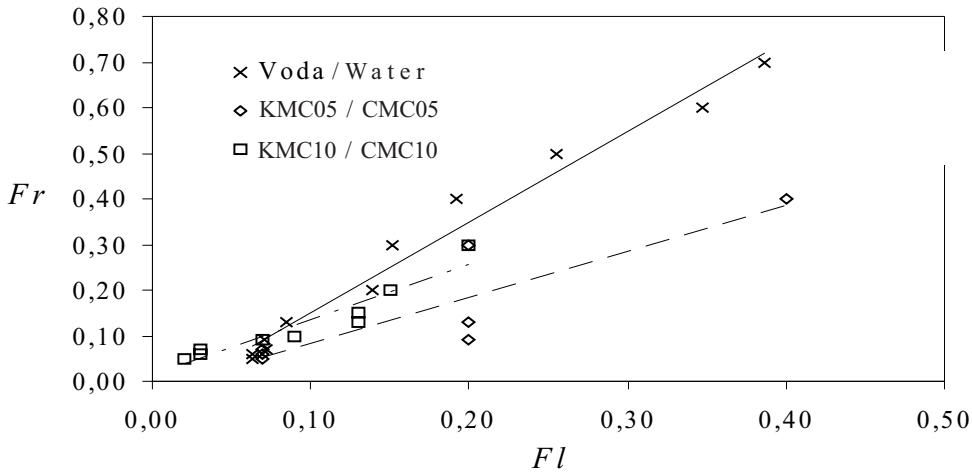


Sl. 14. *Nastanek poplavnega stanja pri dispergiranju zraka v vodo in 0,5% in 1,0% raztopino KMC*
Fig. 14. *Flooding transition in air dispersing into water and into CMC of 0.5 and 1.0 % mass concentration of CMC*

plastični tekočini poteka prehod iz dispergirnega v poplavno stanje prek strukture L6, kar se kaže z nastankom poplavnega stanja pri precej večjih vrednostih pretočnega števila (sl. 14). Primerjave z vrednostmi po virih iz literature zaradi očitnega pomanjkanja tovrstnih podatkov ni bilo mogoče izvesti. Pomembna je ugotovitev, da je porazdelitev plinaste faze po prostornini kapljevine pri 0,5% raztopini KMC še dokaj zadovoljivo, medtem ko dispergiranje v 1% raztopini verjetno že meji na neučinkovito delovanje.

## 3 SKLEP

Obravnavana je bila zaznava poplavnega stanja v posodi z enojnim Rushtonovim mešalom pri dispergiranju zraka v vodi s tremi različnimi metodami, to so: metoda celotnega prirastka plinaste faze, metoda najmanjše moči mešanja in metoda karakteristik faznega stika ter pri dispergiranju zraka

Transition from the dispersing to the flooding state was performed via a structure of six identical large cavities, which was reflected in much higher values of flow number, shown in Figure 14. A comparison with values from literature sources could not be made due to the obvious lack of such data. Another significant finding was that the impeller was capable of dispersing air into fluid at 0.5% of the mass concentration, whereas at 1% of the mass concentration dispersing was seen to be an unsatisfactory operation, in other words, any other impeller suitable for higher viscosities should be used.

## 3 CONCLUSION

In a mixing vessel equipped with a Rushton turbine, the recognition of the flooding state during the dispersion of air into water was detected with three different methods: the global-gas-holdup method, minimum-mixing-power method and the interfacial characteristics method, while for the

v vodni raztopini karboksi – metil celuloze z metodo karakteristik faznega stika.

Narejena je bila primerjava rezultatov posameznih metod in ocena primernosti uporabe posamezne metode za določitev poplavnega stanja. Poplavno stanje mešala je bilo zaznano z vsemi tremi metodami. Glede na to, da je na gredi le eno mešalo, se krajevne spremembe na mešalu kažejo neposredno tudi na celotni ravni. Rezultati vseh treh metod se med seboj dokaj dobro ujemajo, za industrijsko uporabo lahko uporabimo katerokoli od omenjenih metod.

dispersing of air into a CMC solution the interfacial characteristics method was used.

An estimation of the individual method's adequacy, as well as a comparison of the results of the given methods was performed. Impeller flooding was detected by using all three methods. The results of the discussed methods were in good agreement among themselves, as well as with the given criteria and results of other researchers. Any of the mentioned methods can be applied to industrial use. Given the fact that air-dispersing was performed with a single Rushton impeller, all the changes at the local level are reflected directly in the global one.

ZAHVALA

To delo je del večjega projekta J2-7517, ki ga financira Ministrstvo za šolstvo, znanost in šport Republike Slovenije.

ACKNOWLEDGMENT

The authors wish to acknowledge the Slovenian Ministry of Education, Science and Sport for financial support under the current project No. J2-7517.

## 3 OZNAKE
## 3 SYMBOLS

| | | | |
|---|---|---|---|
| premer mešala | $D$ | m | impeller diameter |
| zemeljski pospešek | g | $m/s^2$ | gravity |
| vrtilna frekvenca mešala | $n$ | $s^{-1}$ | impeller rotational frequency |
| moč pri mešanju kapljevine | $P$ | W | impeller power |
| prostorninski pretok zraka | $q$ | $m^3/s$ | volumetric air flow |
| premer posode | $T$ | m | tank diameter |
| pretočno število | $Fl$ | $q/(n \cdot D^3)$ | flow number |
| Froudeovo število | $Fr$ | $D \cdot n^2/g$ | Froude number |
| celotni delež plinaste faze | $\alpha$ | % | global gas holdup |
| razmerje moči | $\pi_i$ | $P_{g,i}/P$ | power ratio |
| **Indeksi:** | | | **Indexes:** |
| tekoči indeks | $i, j$ | | current index |
| poplavno stanje | $F$ | | flooding state |
| dispergiranje plina v kapljevino | $g$ | | dispersing state |

## 4 LITERATURA
## 4 REFERENCES

[1] Bombač, A. (1998) Vpliv geometrijskih parametrov na Newtonovo število pri aeraciji v posodi z mešali, *Strojniški vestnik* (44) 3-4.

[2] Bombač, A. and I. Žun (1992) Detection of loading-flooding transition in an aerated stirred vessel, in Proc. Kuhljevi dnevi, (in Slovene), Portorož, *Slovene Society of Mechanics*, 123.

[3] Bombač, A., I. Žun, M. Žumer, J. Turk (1996) Strukture plinskih votlin pri dispergiranju zraka v psevdoplastično tekočino s turbinskim mešalom, Kuhljevi dnevi, Gozd-Martuljek, *Slovensko društvo za mehaniko*.

[4] Bombač, A., I. Žun, B. Filipič, M. Žumer (1997) Gas-filled cavity structures and local void fraction distribution in aerated stirred vessel, *AIChE J.*

[5] Bombač, A., I. Žun (2000) Gas-filled cavity structures and local void fraction distribution in vessel with dual-impellers. *ChemEngSci*, (55), 15.

[6] Lu, W., H. Chen (1986) Flooding and critical impeller speed for gas dispersion in aerated turbine-agitated vessels, *Chem. Eng. Jour.*, 33.

[7] Nienow, A. W., M. M .C. G. Warmoskerken, J. M. Smith, M. Konno ((1985) On flooding/loading transition and the complete dispersal condition in aerated vessels agitated by a Rushton-turbine, Proc 5th European Conference on Mixing, Wuerzburk, *BHRA Fluid Enginireeng Cranfield*, 143-154.

[8] Rushton, J. H., J.J. Bimbinet (1964) Hold-up and flooding in air-water mixing, *Can J. Chem. Eng.*, 46.
[9] Smith, J. M. (1991) Simple performance correlations for agitated vessels, in fluid mechanics of mixing, ed. R. King, *Kluwer Academic Publisher*, Dordrecht, 55.
[10] Turk, J. (1999) Poplavno stanje pri večstopenjskem turbinskem mešalu, Diplomsko delo, *Univerza v Ljubljani*, FS, Ljubljana.
[11] Warmoeskerken, M. M. C. G. and J. M. Smith (1985) Flooding of disk turbines in gas-liquid dispersions: A new description of the phenomenon, *Chem. Eng. Sci*., 40, No. 11, 2063.
[12] Wiedmann, J.A. (1983) Zum Überflutungsverhalten zwei- und dreiphasig betriebener Rührreaktoren. *Chem.Ing.Tech*., 55, 9.
[13] Žun, I., A. Bombač (1997) An application of local void fraction measurements in discharge flow of single and dual Rushton turbine, *Proc. 9th European Conference on Mixing/Mixing 97/Mutiphase systems*, Paris, 153.

Naslov avtorjev: doc.dr. Andrej Bombač
prof.dr. Iztok Žun
Fakulteta za strojništvo
Univerza v Ljubljani
Aškerčeva 6
1000 Ljubljana
andrej.bombac@fs.uni-lj.si
iztok.zun@fs.uni-lj.si

Authors' Address: Doc.Dr. Andrej Bombač
Prof.Dr. Iztok Žun
Faculty of Mechanical Eng.
University of Ljubljana
Aškerčeva 6
1000 Ljubljana, Slovenia
andrej.bombac@fs.uni-lj.si
iztok.zun@fs.uni-lj.si

Prejeto: 20.12.2002
Received:

Sprejeto: 31.1.2003
Accepted:

© Strojniški vestnik 48(2002)12,677-686
ISSN 0039-2480
UDK 532.7:533.6.08
Izvirni znanstveni članek (1.01)

© Journal of Mechanical Engineering 48(2002)12,677-686
ISSN 0039-2480
UDC 532.7:533.6.08
Original scientific paper (1.01)

# Analiza kinematike toka v rotirajočem difuzorju

## An Analysis of the Flow Kinematics in a Rotating Diffuser

**Tom Bajcar - Brane Širok - Ferdinand Trenc - Dragica Jošt**

*V prispevku so predstavljene raziskave hitrostnega polja toka zraka v rotirajočem vzdolžnem difuzorju okroglega prereza. Meritve hitrostnih komponent toka so potekale z uporabo laser-Dopplerjeve anemometrije (LDA). Z meritvami je bila potrjena delitev toka na zunanji vrtilni del ob vrteči se steni in notranji nevrtilni del v vzdolžni osi difuzorja. Ugotovljeno je bilo pomembno povečanje vseh treh komponent hitrosti v ozkem pasu ob vrteči se steni difuzorja. Poleg tega je bil izveden tudi numerični izračun hitrostnega polja v difuzorju s tremi različnimi turbulentnimi modeli.*

**(Ključne besede: difuzorji rotirajoči, kinematika toka, polja hitrostna, anemometrija Dopplerjeva, anemometrija laserska)**

*This paper describes a study of the flow-velocity field inside a rotating axial diffuser with a circular cross-section. The flow-velocity components were measured with an LDA system. The velocity-component measurements confirmed the existence of two types of flow: a rotating region near the rotating wall and a non-rotating region near the longitudinal axis of the diffuser. A significant increase in all three velocity components was observed in a thin layer at the rotating-diffuser wall. In addition, three different turbulence-closure models were applied for the velocity-field prediction inside the rotating diffuser.*

**(Keywords: rotating diffusers, flow kinematics, velocity fields, laser-Doppler anemometry)**

### 0 UVOD

Analiza hitrostnega polja turbulentnega toka tekočine v vrtečem se vzdolžnem difuzorju ima svoje osnove v raziskavah toka tekočine skozi difuzor in preučevanju vrtinčnih tokov. Začetek pomembnejših raziskav toka v difuzorju sega nekako v prva desetletja 20. stoletja, predvsem z namenom preučiti dogajanje v mejni plasti difuzorja pri različnih kotih razširitve difuzorja [1]. Preveliki koti razširitve namreč povzročijo, da se mejna plast ob steni difuzorja na določenem mestu odlepi od stene, kar je posledica vzdolžnih tlačnih gradientov.

Ena izmed glavnih značilnosti vrtinčnih tokov je pojav centrifugalne sile kot posledice radialnega tlačnega gradienta, ki se pojavi v vrtinčnih tokovih [2]. V najpreprostejši obliki z zanemaritvijo strižnih sil ima radialni tlačni gradient $\partial p/\partial r$ obliko:

$$\frac{\partial p}{\partial r} = \rho \cdot \frac{u_t^2}{r} \qquad (1),$$

kjer so: $\rho$ gostota tekočine, $u_t$ njegova obodna hitrost, $r$ pa radij. Centrifugalna sila pospešuje širjenje curka vrtinčnega toka radialno navzven.

### 0 INTRODUCTION

Analyses of the velocity field of the turbulent fluid flow in an axially rotating diffuser are based on studies of the fluid flowing through a stationary diffuser and on investigations of the swirl flow. Studies of flow inside the diffuser were initiated in the first decades of the 20$^{th}$ century, mainly to investigate the fluid behaviour inside the diffuser's boundary layer at different diffuser cone angles [1]. Diffuser cone angles that are too large cause the boundary layer at a particular point of the diffuser to separate from the wall. This separation is a consequence of the axial pressure gradients.

One of the main properties of the swirl flow is the presence of a centrifugal force, which is a consequence of the radial pressure gradient in swirl flows [2]. The simplest form of the radial pressure gradient $\partial p/\partial r$, where the shear forces are negligible, can be expressed as:

$$\frac{\partial p}{\partial r} = \rho \cdot \frac{u_t^2}{r} \qquad (1),$$

where $\rho$, $u_t$ and $r$ denote fluid density, fluid tangential velocity and radius, respectively. The centrifugal force enhances the swirling flow jet to spread radially outwards.